AFGL-TR-88-0144
ENVIRONMENTAL RESEARCH PAPERS, NO. 1005

AD-A203 984

Blending of Surface and Rawinsonde Data in Mesoscale Objective Analysis

SAMUEL Y. K. YEE

ARTHUR J. JACKSON

14 June 1988

DTIC
SELECTED
1   1989
α E

ATMOSPHERIC SCIENCES DIVISION   PROJECT 6670
AIR FORCE GEOPHYSICS LABORATORY
HANSCOM AFB, MA 01731

89 2 10 078

"This technical report has been reviewed and is approved for publication"

REPORT DOCUMENTATION PAGE

1a. REPORT SECURITY CLASSIFICATION	1b. RESTRICTIVE MARKINGS
Unclassified	

2a. SECURITY CLASSIFICATION AUTHORITY	3. DISTRIBUTION/AVAILABILITY OF REPORT
	Approved for public release;
2b. DECLASSIFICATION/DOWNGRADING SCHEDULE	distribution unlimited

4. PERFORMING ORGANIZATION REPORT NUMBER(S)	5. MONITORING ORGANIZATION REPORT NUMBER(S)
ERP, No. 1005 AFGL-TR-88-0144	

6a. NAME OF PERFORMING ORGANIZATION	6b. OFFICE SYMBOL *(If applicable)*	7a. NAME OF MONITORING ORGANIZATION
Air Force Geophysics Laboratory	LYP	

6c. ADDRESS *(City, State, and ZIP Code)*	7b. ADDRESS *(City, State, and ZIP Code)*
Hanscom AFB Massachusetts 01731-5000	

8a. NAME OF FUNDING/SPONSORING ORGANIZATION	8b. OFFICE SYMBOL *(If applicable)*	9. PROCUREMENT INSTRUMENT IDENTIFICATION NUMBER

8c. ADDRESS *(City, State, and ZIP Code)*	10. SOURCE OF FUNDING NUMBERS			
	PROGRAM ELEMENT NO	PROJECT NO	TASK NO	WORK UNIT ACCESSION NO.
	62101F	6670	10	16

11. TITLE *(Include Security Classification)*

Blending of Surface and Rawinsonde Data in Mesoscale Objective Analysis

12. PERSONAL AUTHOR(S) Yee, Samuel Y.K., and Jackson, Arthur J.

13a. TYPE OF REPORT	13b. TIME COVERED	14. DATE OF REPORT *(Year, Month, Day)*	15. PAGE COUNT
Scientific. Final.	FROM _____ TO _____	1988 June 14	38

16. SUPPLEMENTARY NOTATION

17. COSATI CODES			18. SUBJECT TERMS *(Continue on reverse if necessary and identify by block number)*
FIELD	GROUP	SUB-GROUP	Mesoscale analysis Mesoscale modeling
			Objective analysis
			Boundary Layer

19. ABSTRACT *(Continue on reverse if necessary and identify by block number)*

This report describes a simple technique to blend surface and rawinsonde observations in the planetary boundary layer (PBL) using a Barnes-type objective analysis. The goal is to improve the mesoscale detail of boundary layer input fields for a mesoscale numerical weather prediction model.

The technique makes use of both surface and rawinsonde data in the boundary layer, where it is known that mesoscale details are inadequately resolved by the rawinsonde network and where the influence of the ground surface is strongest. Our challenge is to blend the signals contained in the denser surface observations that capture at least some mesoscale detail with those contained in the boundary layer rawinsonde data. This is accomplished simply by comparing two analyses at the ground, one containing both the rawinsonde-data-resolvable and surface-data-resolvable information and the other, only the rawinsonde-scale information. Differences between these two fields are assumed to be the signals undetected by the rawinsonde network. These mesoscale signals are then incorporated (cont.)

20. DISTRIBUTION/AVAILABILITY OF ABSTRACT	21. ABSTRACT SECURITY CLASSIFICATION
☒ UNCLASSIFIED/UNLIMITED ☐ SAME AS RPT ☐ DTIC USERS	Unclassified

22a. NAME OF RESPONSIBLE INDIVIDUAL	22b. TELEPHONE *(Include Area Code)*	22c. OFFICE SYMBOL
Samuel Y.K. Yee	(617) 377-2128	LYP

DD FORM 1473, 84 MAR
83 APR edition may be used until exhausted
All other editions are obsolete

SECURITY CLASSIFICATION OF THIS PAGE

Unclassified

Block 19 (cont.).

into the PBL analyses as a function of the distance from the ground.

Results show a positive impact on boundary layer analyses due to the blending of surface and rawinsonde data, demonstrating that the technique is useful for providing improved mesoscale detail at and near the ground.

Also discussed is the relative impact of data density and reference topography on the analysis of model parameters on terrain-following surfaces.

Preface

We would like to thank Donald A. Chisholm and H. Stuart Muench for the use of their objective analysis algorithm, and Audrey Campana and Anna Tortorici for their able assistance in preparing the manuscript.

Contents

Illustrations

Tables

Blending of Surface and Rawinsonde Data in Mesoscale Objective Analysis

I. INTRODUCTION

In mesoscale modeling, emphasis is placed on phenomena in the planetary boundary layer (PBL), phenomena that typically have temporal scales of less than 6 hours and spatial scales of less than 100 km. If the purpose of the modeling is to simulate mesoscale features due to external forcing or internal dynamic adjustments--primarily a boundary-value problem--then realistic specification of initial conditions may be of little concern. Examples of this kind of study range from the use of a single-station sounding[1] to soundings provided by the rawinsonde network.[2] However, if the purpose of the modeling is to predict short-range weather changes--an initial-boundary-value problem--then the ability to represent mesoscale features in the initial conditions becomes important. While data density on the order of the current and planned rawinsonde network may be adequate in specifying large-scale dynamics in the free atmosphere, it is unquestionably inadequate in resolving phenomena in the planetary boundary layer. Since surface observa-

---

1. Nickerson, E. C. (1979) On the numerical simulation of airflow and clouds over mountainous terrain, Beit. zur Physik der Atmos. 52:161-177.

2. Perkey, D. J. (1976) A description of preliminary results from a fine-mesh model for forecasting quantitative precipitation. Mon. Wea. Rev. 104:1513-1526.

1

tions, due to their high spatial and temporal resolutions, provide valuable information about the planetary boundary layer, every effort should be made to include these surface reports in a mesoscale analysis-forecasting system. Perhaps for this reason, care has been taken to include certain surface observations over land in regional and mesoscale analyses.[3,4,5]

In this report, we present a simple method that blends, in a Barnes-type objective analysis, observations from both rawinsonde and surface stations. The method is based on the following idea: Although radiosonde observations have poor horizontal and temporal resolutions, they do have fairly good vertical resolution, particularly near the surface. Similarly, while surface reports have no vertical resolution at all, their horizontal and temporal resolutions are much higher than those of the rawinsonde network. We may, therefore, exploit the complementary nature of these two sets of observations to capture PBL mesoscale features in, for example, the boundary layer analyses of temperature T, specific humidity q, and the two horizontal components of the wind u and v. This idea can be put to the test in practice in many ways. We choose here to incorporate signals in the difference-field of two surface analyses, one containing only surface reports from rawinsonde stations, the other, surface reports from a denser network. A description of this blending method is given in Section 2. The procedure used in carrying out this technique is outlined in Section 3. Sample results, which, by and large, show a positive impact of the blending on the analyses, are presented in Section 4. The advantages, disadvantages, implications, and generalization of the blending approach adopted are discussed in Section 5.

2. BLENDING TECHNIQUE

Our primary goal is to obtain, from conventional rawinsonde soundings and surface reports, analyses that depict realistic mesoscale features in the boundary layer. We shall, however, limit the scope of our study to two-dimensional univariate objective analysis on terrain-following constant σ-surfaces. The pros and cons of analyzing observations on such surfaces will be discussed later. Consider first the case where observations are analyzed one level at a time. In this case,

3. DiMego, G. J. (1988) The National Meteorological Center regional analysis system, Mon. Wea. Rev. (in press).

4. Golding, B. W. (1987) Strategies for using mesoscale data in an operational mesoscale model, in Mesoscale Analysis and Forecasting. Proc. IAMAP/WMO/ESA, Vancouver, Canada, pp. 569-578.

5. Gustafsson, N. (1987) Opportunities and problems in mesoscale analysis, in Mesoscale Analysis and Forecasting. Proc. IAMAP/WMO/ESA, Vancouver, Canada, pp. 555-560.

surface analyses will contain mesoscale features while analyses for any level above the ground will retain only features that can be resolved by the rawinsonde network. Due to the difference in observational density, the two sets of analyses are, therefore, strictly speaking, incompatible. For this and other reasons, surface reports have been mostly excluded from global analysis. For mesoscale analyses, attempts have been made in the past to blend surface and rawinsonde observations in Barnes-type analyses for the boundary layer. For example, Kalb[6] used hourly surface wind data to construct low-level wind fields for a boundary layer of approximately 2 km in depth. He obtained u and v components of the wind in the boundary layer by linearly interpolating between analyzed winds at the surface and at a model level located at about 2 km above the ground. An Ekman-type turning of the winds with height in the boundary layer was thus effected. In this method, rawinsonde data in the boundary layer were discarded, however.

The method we describe below shall make use of both the surface data and rawinsonde data in the boundary layer. In this approach, we pre-suppose that there exists a level in the atmosphere above which the atmosphere is adequately sampled by the rawinsonde network. For the atmosphere below this level, which we have referred to rather loosely as the boundary layer, meteorological signals are not fully resolved by the rawinsonde network. Our challenge is to blend the signals contained in the denser surface observations with those contained in the boundary layer rawinsonde data. This we accomplish simply by comparing two analyses at the ground surface, one retaining both the rawinsonde-data-resolvable and surface-data-resolvable information, and the other, only the rawinsonde-scale information. The differences between these two analyses are assumed to be the signals undetected by the rawinsonde network. Our task is to incorporate in the PBL analyses these mesoscale signals as a function of the distance from the ground.

We shall adopt a vertical coordinate σ that is related to the atmospheric pressure p by

$$\sigma = (p - p_T)/(p_S - p_T) \tag{1}$$

where p_S, p_T are pressures at the model lower and upper boundaries, respectively. Here, p_S is a function of the horizontal coordinates (x, y) as well as time t; but p_T is a prespecified constant, independent of (x, y, t). Furthermore,

---

6. Kalb, M. W. (1984) Initialization of a mesoscale model for April 10, 1979, using alternative data sources. NASA Contractor Report 3826, NASA, D. C. 20456.

we shall choose our model vertical structure in a certain way and conduct analyses only on σ-surfaces specified by

$$\sigma_k = \frac{(4\nu_k - \nu_k^4)}{3} \;.$$

(2)

Here $\nu_1 = 1$, and a constant $\Delta\nu$ is used to define $\nu_k = 1 - (k - 1.5)\Delta\nu$, k being an integer greater than 1. An advantage of specifying the σ_k structure this way is that, for a constant increment $\Delta\nu$, more computational levels (higher resolutions) are packed near the ground. A typical model vertical structure with $\Delta\nu = 1/15$ is given in terms of ν, σ and p in Table 1.

Table 1. Sample Model Vertical Structure ($\Delta\nu = 1/15$, Surface Pressure = 979 mb)

k	ν_k	σ_k	$\bar{p}_k$(mb)
16	0.03	0.04	139
15	0.10	0.13	217
14	0.17	0.22	295
13	0.23	0.31	373
12	0.30	0.40	449
11	0.37	0.48	524
10	0.43	0.57	598
9	0.50	0.65	668
8	0.57	0.72	734
7	0.63	0.79	795
6	0.70	0.86	850
5	0.77	0.91	897
4	0.83	0.95	935
3	0.90	0.98	963
2	0.97	1.00	977
1	1.00	1.00	979

If the location at x_i, y_j, and σ_k is represented by (i, j, k), then the analysis of a data set, say that of rawinsonde temperature, may be represented by $T_{i,j,k}$. Now let $T_{i,j,1}$ and $TS_{i,j}$ be two temperature analyses at the ground, the former containing only surface data from the rawinsonde network, the latter containing additional surface observations from a denser network; and let the difference of the two analyses be

$$D_{i,j} = TS_{i,j} - T_{i,j,1}.$$ (3)

Our task, simply put, is to make use of $D_{i,j}$ to modify the analyses $T_{i,j,k}$ for $k \le L$, L being the level above which the surface inference is assumed to be small. Thus, we may, for example, modify $T_{i,j,k}$ to yield

$$T_{i,j,k} = T_{i,j,k} + W_k D_{i,j} \qquad\qquad 1 \le k \le L.$$ (4)

Where $T_{i,j,k}$ is the modified analysis and W_k is a weighting factor that is a function of k only. With the exception of the constraints $W_1 = 1$ and $W_L = 0$, the form of W_k is unspecified. In practice, W_k may be modeled empirically to take on a different set of values for a different variable. In our tests, we simply assume that W_k is linear in ν: $W_k = (\nu_k - \nu_{L+1})/(1 - \nu_{L+1})$.

3. IMPLEMENTATION PROCEDURE

We have tested the technique described above with a data-denial type numerical experiment for the domain shown in Figure 1. This analysis domain, encompassing parts of Oklahoma and most of Texas, was chosen to take advantage of an excellent series of 3-hourly, dense-network data sets for the 18-hour period beginning 12z, 27 March 1982. These data were collected by NASA as part of the AVE/VAS Ground Truth Field Experiments.[7] As shown in Figure 1, 7 conventional rawinsonde stations and 14 special sounding stations were in operation within this domain. The average station-separation was about 400 km for the former and about 100 km for the latter. In our study, we generally make two "parallel-twin" analyses, one containing only data from the former network and the other data from the combined dense-network. Analyses of data from the latter, which we call "the truth," are considered the control runs. In the rest of this report,

---

7. Scienkiewicz, M. E. (1982) AVE/VAS III: 25 mb Sounding Data. NASA Contractor Report 170692, NASA, D.C. 20456.

5
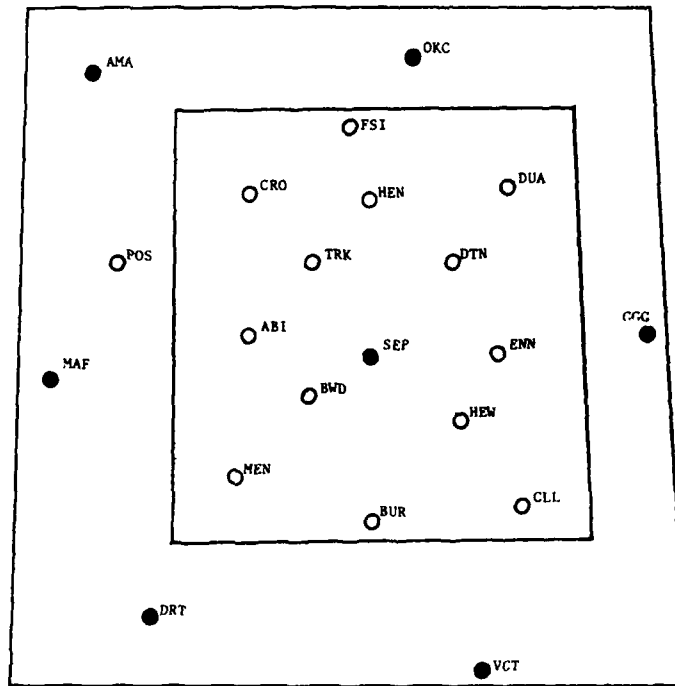
Figure 1. The Analysis and Verification
Domain

when we use the term "surface data," we specifically mean surface data contained
in this data set only. Although additional surface data from other National Wea-
ther Service (NWS) stations were available to our study, they are not presented
here because we want to focus on the comparison between the unmodified and the
blended analyses with the control analyses.

A two-pass Barnes-type objective analysis scheme[8] is applied with a grid-
spacing of about 50 km to the 12z 27 March 1982 observations. These analyses
are then bilinearly interpolated for the region inside the smaller inner grid shown
(about 500 km to the side with a 20 km grid resolution). Comparison of analyses
will be limited to the gridded values within the smaller grid. We shall discuss in
this section first problems associated with constant σ-surface analysis and then
the computational detail of implementing the blending technique.

3.1 Analysis on Constant Sigma-Surface

In spite of the widespread use of the so-called σ-coordinate in NWP models,
until fairly recently, objective analysis for these models has been conducted

---

8. Muench, H. S., and Chisholm, D. A. (1985) Aviation Weather Forecast Based
    on Advection: Experiments Using Modified Initial Conditions and Improved
    Analyses. AFGL-TR-85-0011, AD A160369.

6

largely on constant pressure surfaces. The current trend in operational meso-scale models, however, is toward analyzing initial conditions on constant σ-sur-faces.[5] In this approach, soundings are interpolated from the p-coordinate to the model σ-coordinate and then analyzed directly on the model's σ-surfaces. The motivating force behind this shift in practice seems to be the realization that the use of analysis surfaces that coincide with the model prognostic surfaces will eliminate the need for repeated vertical interpolations in the four-dimensional data assimilation cycle of an analysis-forecast system, and the reduction of inter-polation errors that result. However, to analyze on a constant σ-surface, we im-plicitly assume a surface pressure analysis defined on an analyzed topography grid that is a function of the elevation of the participating observational sites and is, therefore, time-dependent! In practice, model gridded ground elevations are considered to be time-independent, specified from values archived by, say, the U.S. Defense Mapping Agency. This is, of course, just another way of stating one of the time-honored concerns about analyzing observed data at the ground surface where $\sigma = 1$. Near steep mountain ranges, for example, analyzed "surface" val-ues at model grid points may not, in fact, be located at the ground at all--how far above or below the ground at a given grid point depends on the number and the geo-graphical location of the data points.

A specific example of this is given in Figure 2, which depicts three different renditions of the ground elevation along a straight line running from the west to the east near the southern boundary of our verification domain. Here the solid line represents the time-independent archived ground elevation that we shall refer to as "the truth." The analyzed ground elevation is represented by the dotted line for the case where all 21 stations are included in the analysis, and by the dashed line if only the elevations from the 7 NWS stations are used. Since the analysis of surface observations must be considered to be located at the analyzed ground elevations, this figure is important not only because it shows that the reference ground surface is a function of the number and location of observing sites; but also because it clearly demonstrates that the analysis of a parameter is to be measured with respect to a ground surface which, as a general rule, does not coincide with the archived ground surface.

Thus, the first task of our study is to determine accurately the surface pres-sure at the archived elevation (ZZ) of the analysis grid. The following is a proce-dure aimed at attaining such a goal:

a. Analyze the reported surface pressure, temperature, and station elevation to obtain gridded values p_Z, T_Z, and Z, respectively.

b. Compute the difference between analyzed and archived elevations:

$$\Delta Z = Z - ZZ \tag{5}$$

7
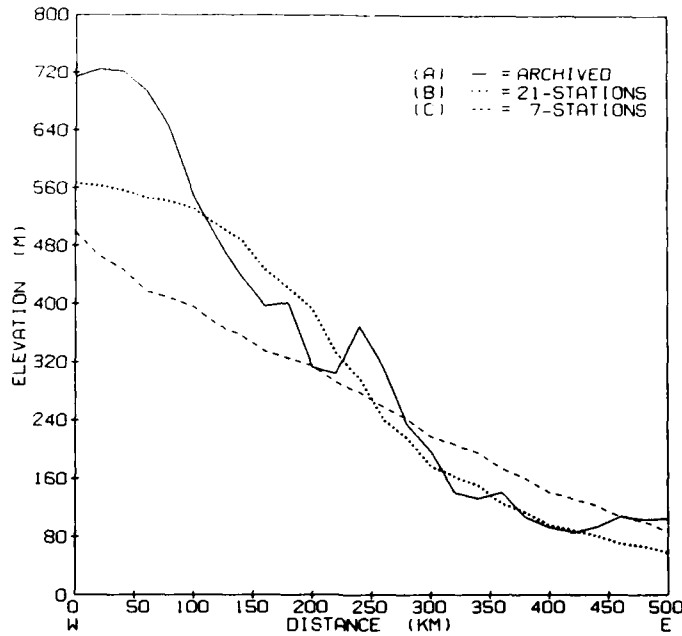
Figure 2. Three Renditions of the Ground
Elevation Along the Southern Boundary of
the Verification Domain

c. Estimate temperature at <u>archived</u> elevations:

$$T_{ZZ} = T_z + \gamma \Delta Z \tag{6}$$

where $\gamma = - \delta T / \delta Z$ is set here to be $6.5 \, \mathrm{K \, km^{-1}}$.

d. Estimate pressure at <u>archived</u> elevations:

$$p_{ZZ} = p_Z \exp [g \Delta Z / (R\overline{T})] \tag{7}$$

where $\overline{T} = (T_Z + T_{ZZ})/2$, g is the gravity, and R is the universal gas constant. There are two advantages of obtaining an estimate for p_{ZZ} this way: (1) All surface reports are used in the analysis, and (2) the extrapolation upward or downward from Z to ZZ is generally over a relatively short vertical distance ΔZ.

After gridded values of p_{ZZ} are obtained, all constant σ-surface analyses must now be adjusted from the σ-surfaces defined by p_Z to σ-surfaces anchored to p_{ZZ}. This can be accomplished by vertical interpolation at each grid point (i, j). For example, since at a given σ_k, $p_k(Z)$ is related to p_Z by

$$p_k(Z) = p_T + \sigma_k (p_Z - p_T) \tag{8}$$

8

whereas $p_k(ZZ)$ is related to p_{ZZ} by

$$p_k(ZZ) = p_T + \sigma_k(p_{ZZ} - p_T), \tag{9}$$

and since analyses at σ_k are located at the $p_k(Z)$ defined by Eq. (8), we must interpolate the analyses from $p_k(Z)$ to the $p_k(ZZ)$ given by Eq. (9).

At this point, it is appropriate to review the reasons why objective analyses of surface pressure and temperature have been carefully avoided in the past. In addition to the difficulties mentioned above, there are also questions about the representativeness of surface reports and the usefulness of such analyses as a means of depicting weather systems. After all, in regions of steep terrain, the predominant component of surface pressure and temperature variations is due to variations in surface elevations. Analyses at the ground surface, therefore, do not depict the intensity of weather systems effectively. The question of representativeness of surface reports falls outside the scope of the present study. The problem of topographical signals masking atmospheric signals is indeed a problem when human visual interpretation is needed; but it is not a problem when these analyses are used for numerical model ingestion. What is at issue here is that we should make the best use of meteorological signals associated with small-scale (and sometimes large amplitude) variations of the Earth's topography in regions of significant terrain. It is these topographical variations that we attempted to account for, using Eqs. (6) and (7) in the case of surface analyses T_{ZZ} and p_{ZZ}, and using Eqs. (8) and (9) to interpolate from $p_k(Z)$ to $p_k(ZZ)$ in the case of analyses located at model levels above the ground.

3.2 Computational Detail

With the mechanism of adjusting analyses from a σ-coordinate defined by p_Z to a σ-coordinate anchored to p_{ZZ} in place, we are now ready to implement the blending technique. A step-by-step procedure is given below. For the purpose of discussion, we use temperature as an example, but the procedure is applicable to other model parameters such as q, u, and v.

    a. Obtain p_{ZZ} for the combined 21 station network via Eq. (7) in the manner described in Section 3.1.

    b. Interpolate each of the 21 soundings of T, q, u, and v from the reporting pressures to pressures corresponding to model σ-surfaces, based on the surface pressure at the sounding site.

    c. Analyze the 7 NWS station pressure and the rawinsonde data obtained from step (b) on each model σ-surface. These analyses will be known as the 7-station

analyses. The gridded analysis of station pressure is denoted, for example, by $p_z(7)$.

d. For each (i, j), use Eqs. (8) and (9) to adjust analyses from the σ-coordinate defined by $p_z(7)$ to the σ-coordinate anchored to p_{ZZ}. If $p_z(7) < p_{ZZ}$, we must extrapolate to get $T_{i,j,k}$ at p_k between $p_z(7)$ and p_{ZZ}. In this case, a vertically averaged (over the lowest three layers) local lapse-rate from the 7-station analyses is used for the extrapolation.

e. Analyze the 21-station combined-network data obtained from step (b) on each model σ-surface. These analyses will be known as 21-station analyses.

f. Adjust the 21-station analyses in a manner similar to that described in step (d). These results will be known as "the truth."

g. Compute $D_{i,j}$ via Eq. (3).

h. Compute $T'_{i,j,k}$ via Eq. (4) for $1 \leq k \leq L$, where L is set to 5. These results will be known as blended analyses.


4. RESULTS

### 4.1 Impact of Data Density and Reference Topography

The idea of blending surface observations with radiosonde data is based on the premise that the complementary nature of the two will enable us to obtain more accurate analyses in the boundary layer than using radiosonde data alone. Because the number of available surface data and that of upper-air observations at any given time are usually different from each other, we shall discuss first the effect of observational density on an analysis. We have already seen the difference between a 7-station and a 21-station analysis of the ground elevation in a vertical cross-section given in Figure 2. A tentative impression from this figure is that the 7-station analysis is smoother than the 21-station analysis, but the latter is a closer approximation to "the truth" than the former. This impression will be reinforced if we examine the contour maps given in Figure 3. Here, the 7-station analyzed, the archived, and the 21-station analyzed ground elevation fields in decameters are given in panels A, B, and C, respectively. The difference between A and B and that between C and B are given as panels D and E, respectively. Even a casual glance at these panels will reveal that the 21-station analysis is a better approximation to "the truth" than the 7-station analysis. However, the important point here is not so much the vivid demonstration of what has been widely known: An analysis of a rapidly varying parameter for a given domain is strongly dependent on the number and the distribution of available data points. What is important is that, in the so-called σ-surface analysis, the ground surface is the σ-surface to which all other σ-surfaces are to be anchored. A set of
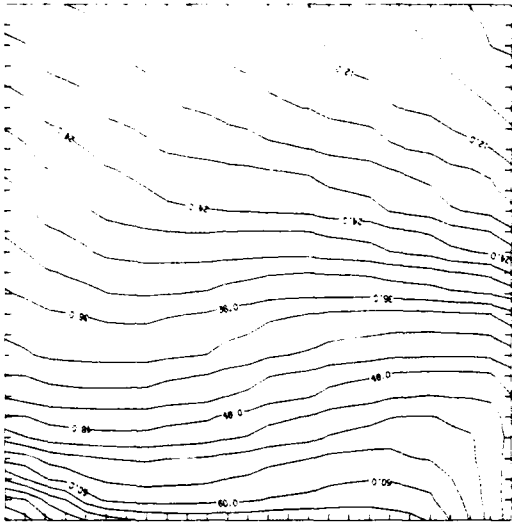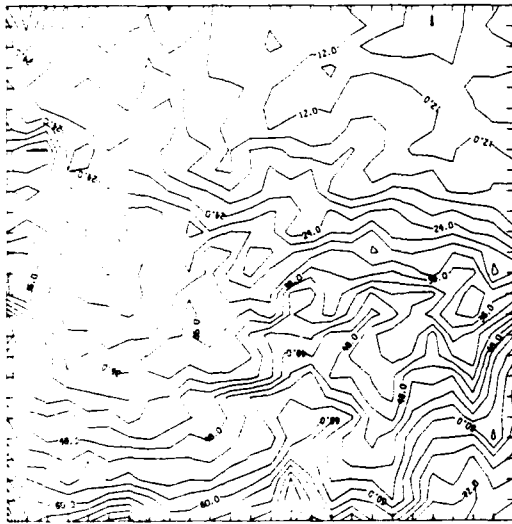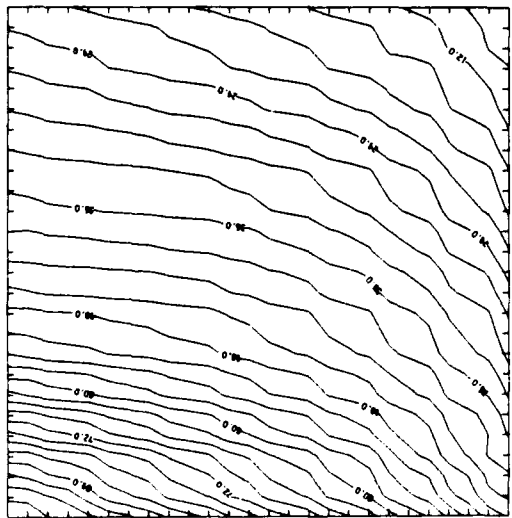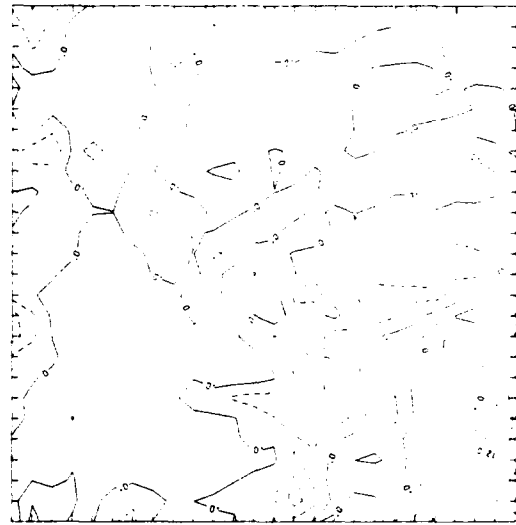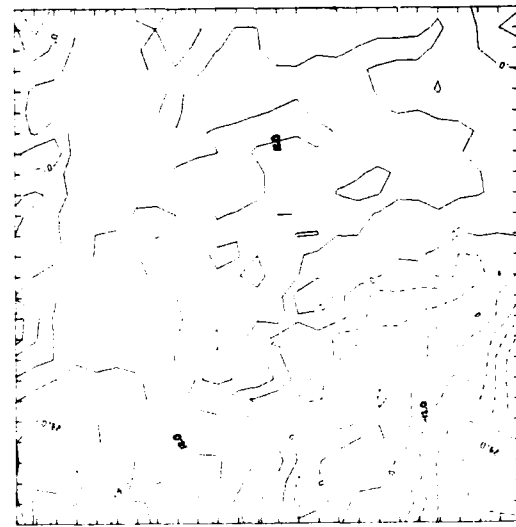
Figure 3. Comparison of Analyzed and Archived Ground Elevation (decameter)

11

gridded values obtained by objectively analyzing N observations at a given σ-surface must be measured with respect to the ground surface obtained by analyzing the elevations at the same N observing stations. If the archived surface topography is to be adopted as the gridded lower boundary of a model, then gridded analyses based on a set of observed data at a given σ must be adjusted for the difference between the topography obtained by analyzing the station elevations and the archived surface topography.

Figures 4, 5, and 6, which depict analyses of surface reports of p, T, and u, respectively, are examples of the case in point. Here, panels A and B are analyses with respect to the <u>analyzed</u> ground elevations based on the station heights of the 7 and 21 reporting stations, respectively. Panels C and D are the same analyses adjusted to the <u>archived</u> elevations. If we compare A with B, or C with D, we get a feel for the impact of data density. On the other hand, if we compare A with C, or B with D, we see the effect of the choice of a reference topography. Note that although the surface pressure analyses shown in panels 4A and 4B differ significantly, panels 4C and 4D (7-station analysis adjusted to ground and 21-station analysis adjusted to ground, respectively) are quite similar, demonstrating the validity of the process used to adjust analyzed surface pressures to the ground. In Figure 5, and more dramatically in Figure 6, significant differences are seen between the 7-station and 21-station unadjusted analyses (panels A and B) and in the 7-station and 21-station adjusted analyses (panels C and D), indicating that data density is quite important in analyzing temperature and winds because local effects typically influence temperature and winds more significantly than pressure.

For the current radiosonde network density in the southwestern part of the United States, it appears from these analyses that an increase in the number of observing stations and the adjustment to the ground surface (archived at 20 km resolution) of an analysis of surface reports are both important. A comparison among panels within each of these figures also reveals clearly why historically analyses of pressure and temperature at the ground have been carefully avoided. In the first place, the effects of data density and of the location of an observation are much stronger near the ground where rapid local variations are the rule. In the second place, a very strong component of the grid point to grid point variations is due to height variations of the ground surface. In fact, in the case of surface pressure, meteorological signals in mountainous regions are clearly masked by the variation of pressure with height. Based on analyses such as these, meteorologists have invented the fictitious sea-level pressure and temperature analyses and the 1000 mb height analysis to remove the strong falloff of pressure and temperature with height. However, if σ-surface analyses are to be used in a NWP model, particularly in a mesoscale model where fine vertical resolution near the
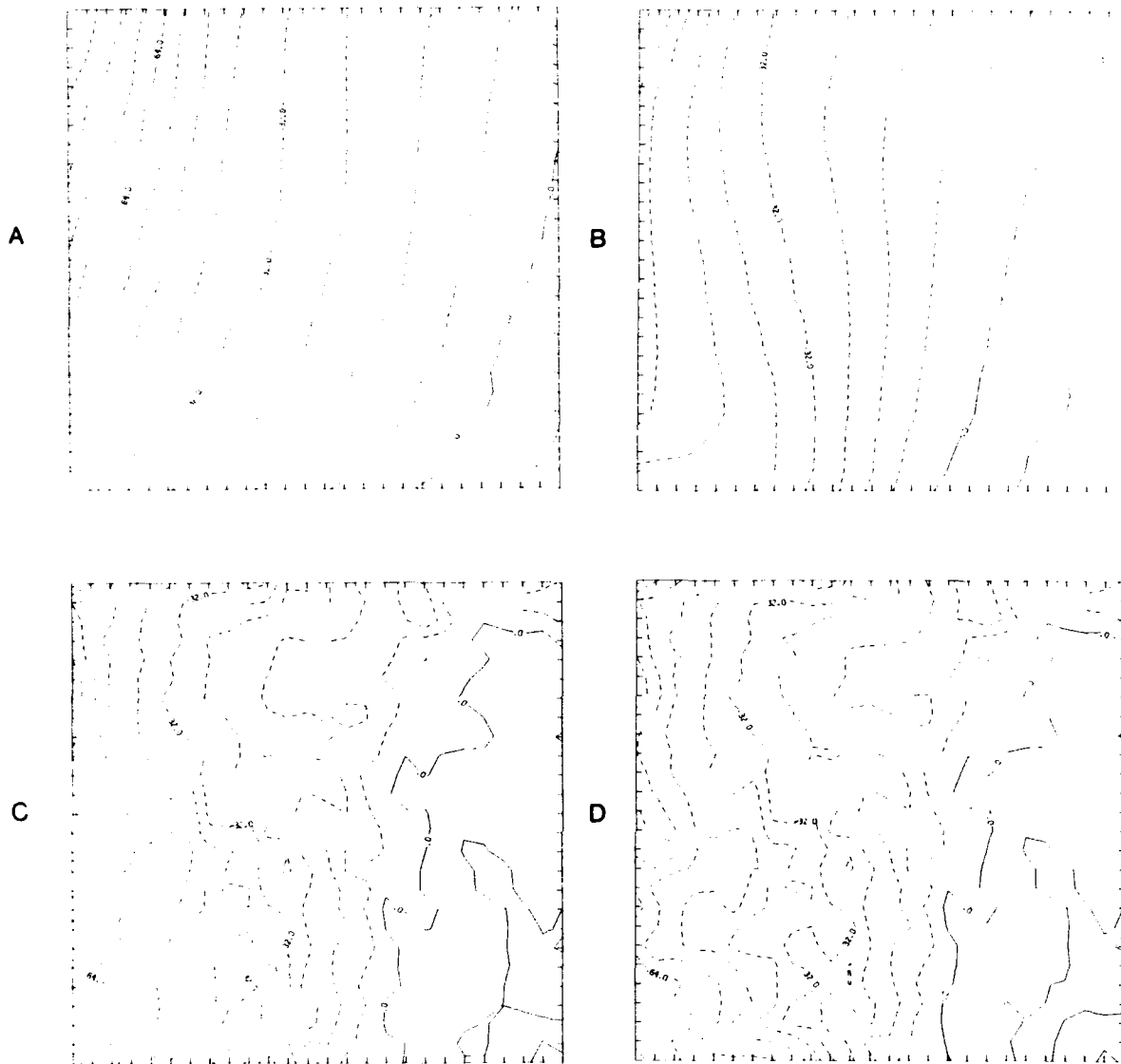
Figure 4. Comparison of Surface Pressure Analyses for 12Z, 27 March 1982
With Respect to Analyzed and Archived Elevation. (Contours are given as
deviations from 1000 mb)

ground is mandated, we must analyze surface data the same way we analyze ob-
served data at any other chosen σ-surfaces in order to be consistent.

We shall next attempt to separate the effect of data density from that of local
topography in our surface pressure and temperature analyses. This is done
graphically in Figures 7 and 8, which are the difference fields among the analyses
given in Figures 4 and 5, respectively. The difference between a 7-station unad-
justed and a 21-station adjusted analysis, labeled panel A, represents the com-
bined effects of data density and reference topography. Figures 7A and 8A both
show significant combined impact on the surface analyses: differences ranging

13
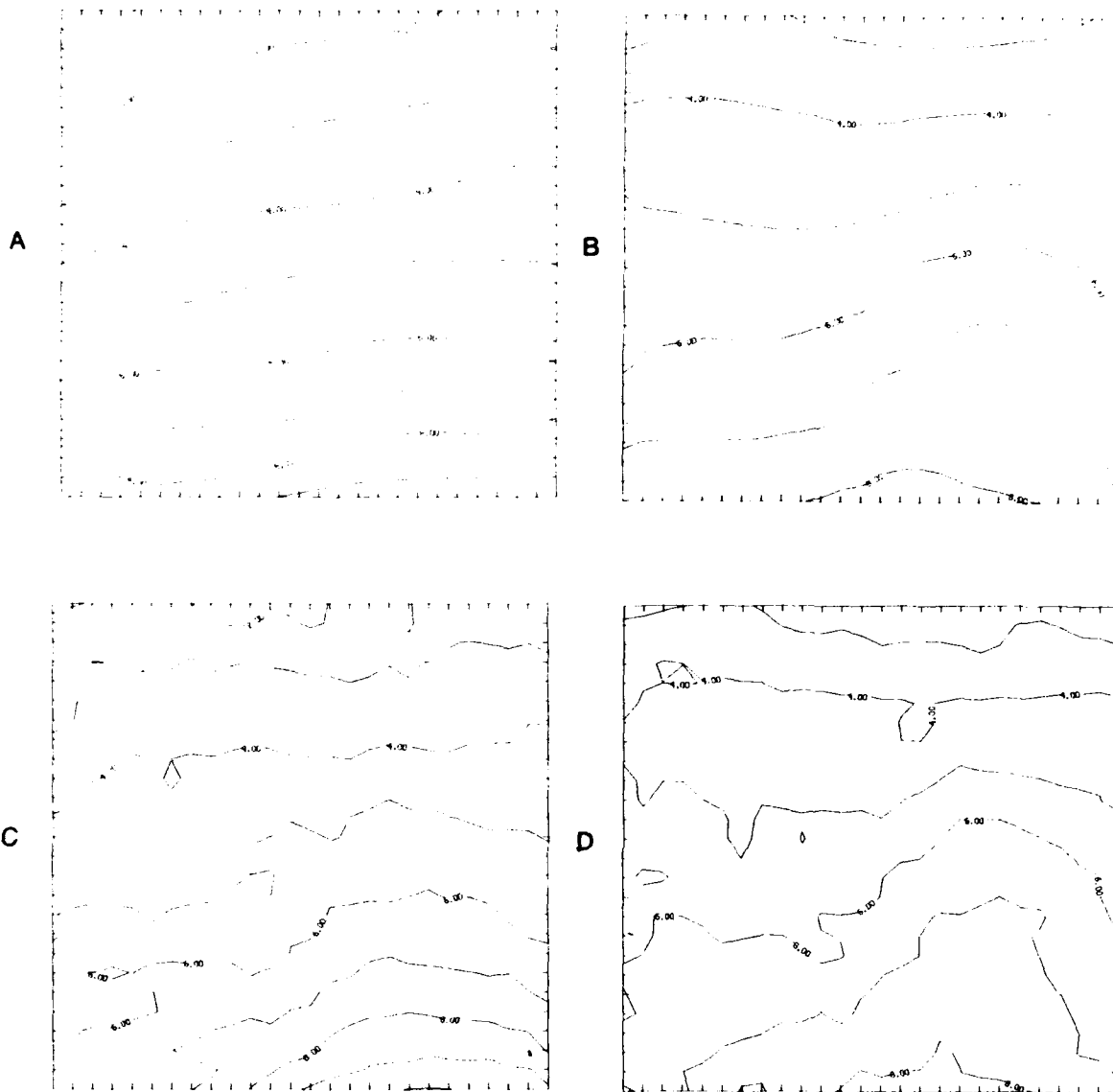
Figure 5. Comparison of T (°C) Analyses for 12A, 27 March 1982, With Respect to Analyzed and Archived Elevation

between ±32 mb in the case of pressure analyses and differences ranging between ±2° C in the case of temperature analyses. These combined effects may be separated into components: that due to data density (the difference-field between panels C and D in Figure 4, shown in panel B) and that due to reference topography (panels C and D, which are difference-fields between Figures 4A and 4C, and between Figures 4B and 4D). We see that panel B is smoother than C and D, suggesting that, in this region, adjustments for local topography may introduce more local features than reducing the average observing station-separation from about 400 km to about 100 km, at least for the σ-surface analyses close to the ground.

14
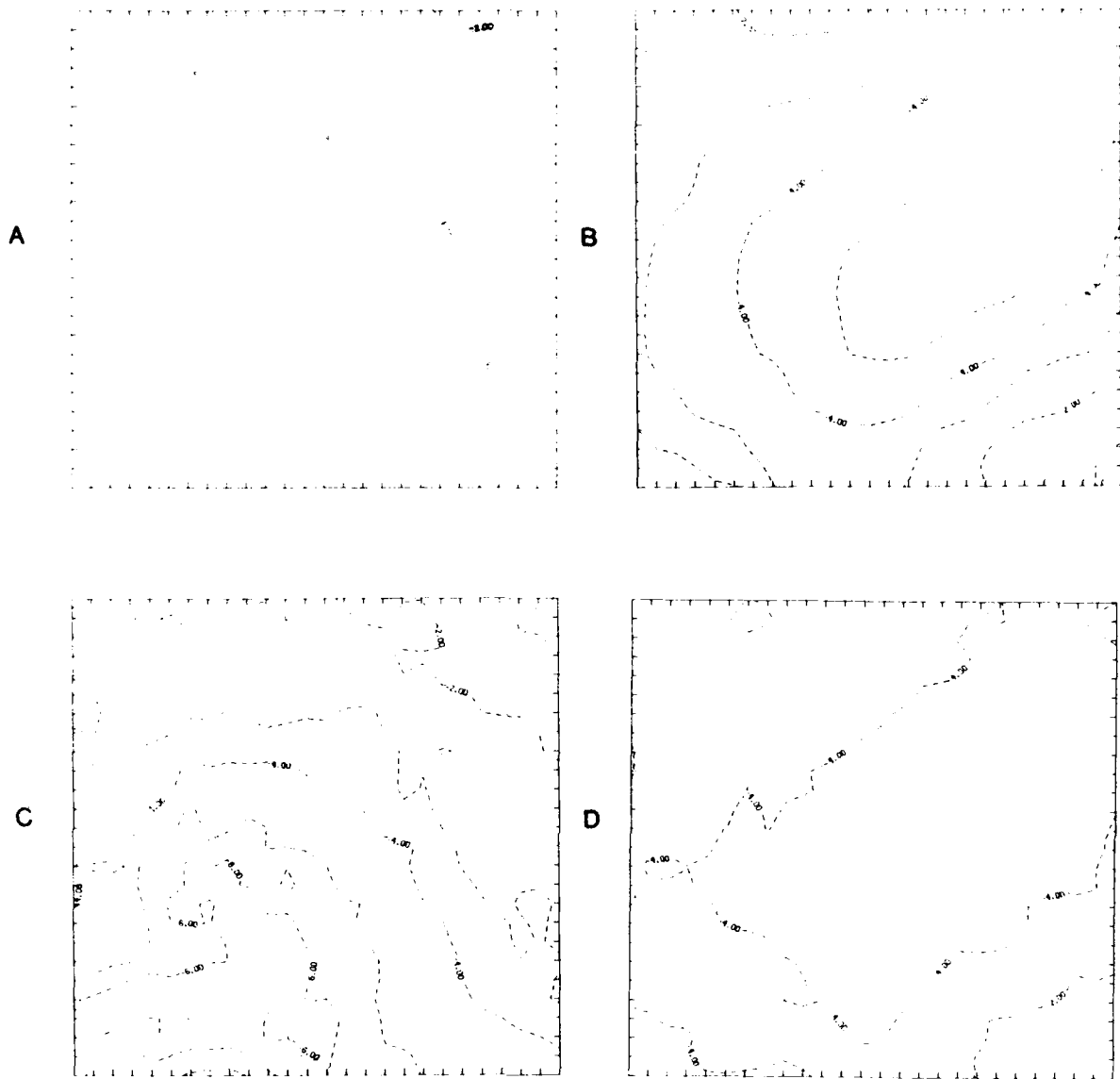
Figure 6. Comparison of u (m/s) Analyses for 12Z, 27 March 1982, With Respect to Analyzed and Archived Elevation

Counter-examples of this can be found in the southeastern corner of our verification domain where the effect of data density outweighs that of reference topography, as can be seen by comparing Figures 8B and 8C. However, this is a region where the ground is relatively flat. Thus, our statement generally holds true except in areas where the local topography is relatively flat so that the horizontal scale of temperature-variation is smaller than that of topographical variation.

Before leaving this subsection, we wish to note again the impact of adjusting the analyzed pressure to the ground. This can best be seen by comparing the impact of data density with that of reference topography in Figures 7B and 7C. The former shows a maximum range of differences of only about ±2 mb; whereas the

15
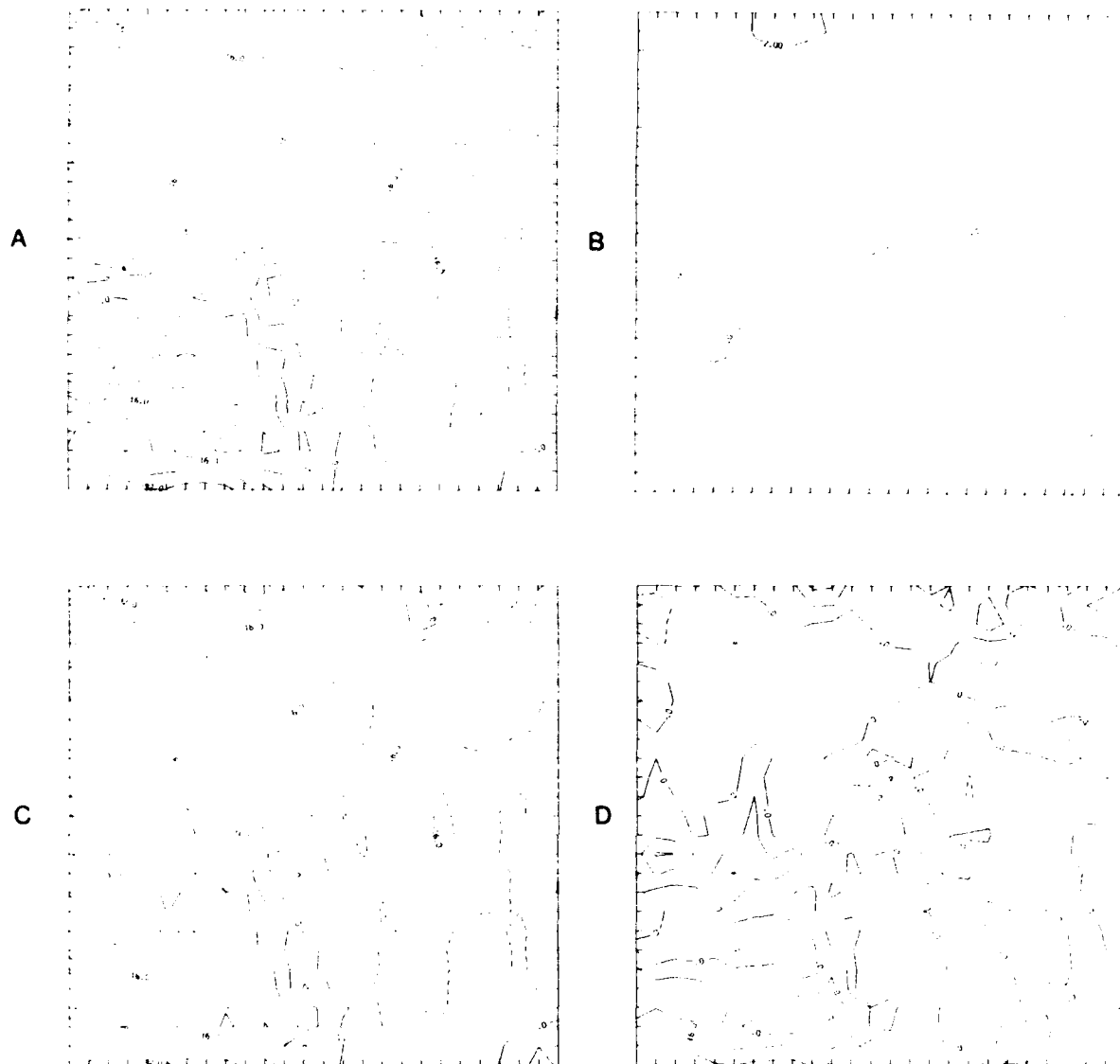
Figure 7. Impact of Data Density (B), Reference Topography (C and D), and the Combined Effect (A) on Surface Pressure Analysis (mb)

latter shows maximum differences of about ± 32 mb. This is important because the grid-point pressure at a given model σ-surface is dependent on the gridded value of the pressure field at the ground.

4.2 Impact of Surface Data

Let us now turn our attention to the effect of blending surface data with radio-sonde observations. We shall do this by intercomparing (in Figures 9, 10, and 11) the 7-station unadjusted analysis (panel A), the blended analysis (panel C) and "the truth" (panel B) of T at the ground (Figure 9), at 150 m (Figure 10) and 700 m
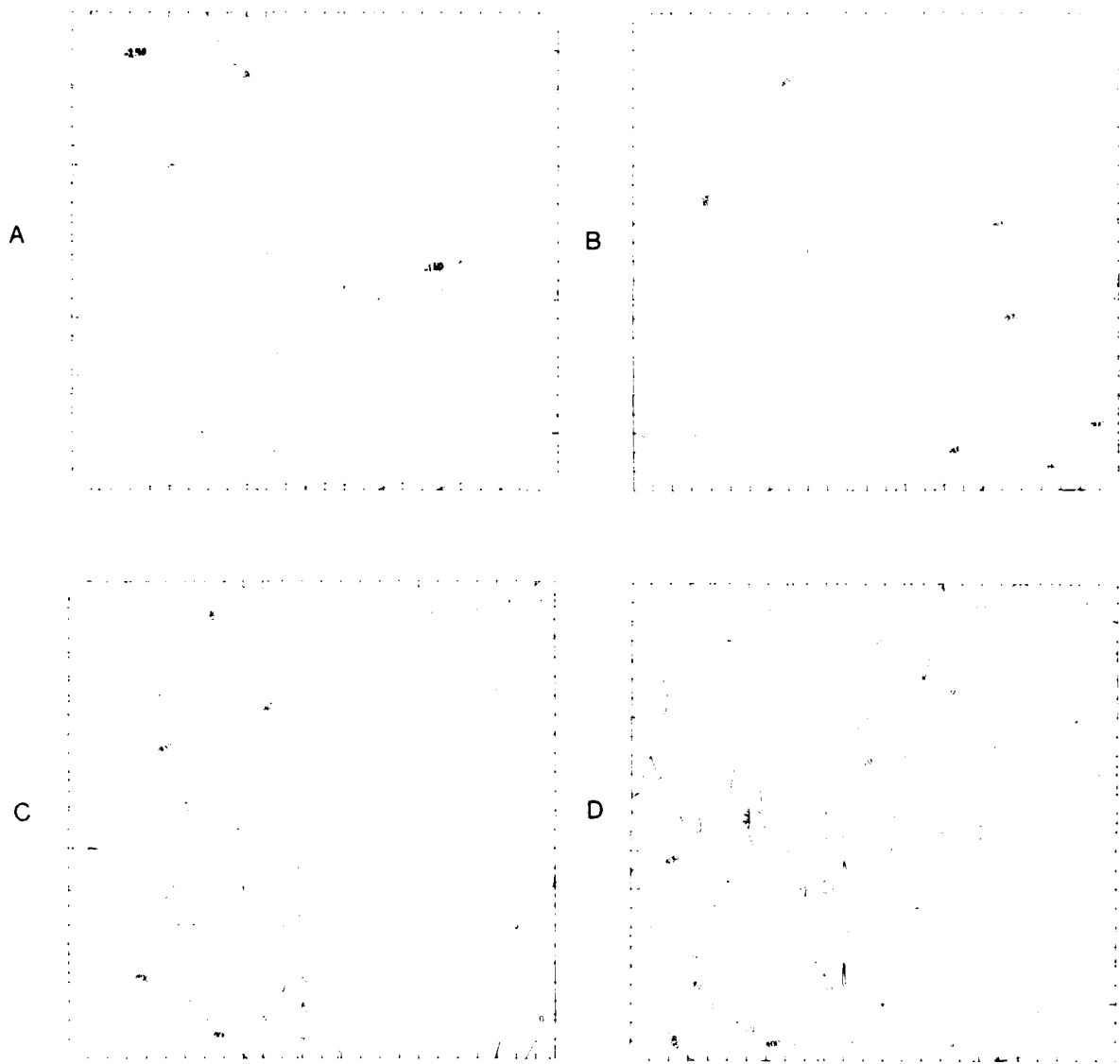
Figure 8.   Impact of Data Density (B), Reference Topography (C and D),
and the Combined Effect (A) on T (° C) Analysis

(Figure 11) above the ground.   Panel D represents the error field of the unadjusted
analysis (panel A - panel B) and panel E represents the error field for the blended
analysis (panel C - panel B).   These figures, corresponding to σ-levels 1, 3, and
5, respectively, are shown to demonstrate that the blending technique is capable
of providing better mesoscale detail at and near the ground and that the influence
of surface data decreases with height.   It is apparent from these figures that the
blended analysis is closer to "the truth" than the 7-station analysis.   For example,
in the case of the temperature analysis in Figure 10, while the unadjusted analysis
exhibits small amplitude (smooth) long waves with relatively strong north-south
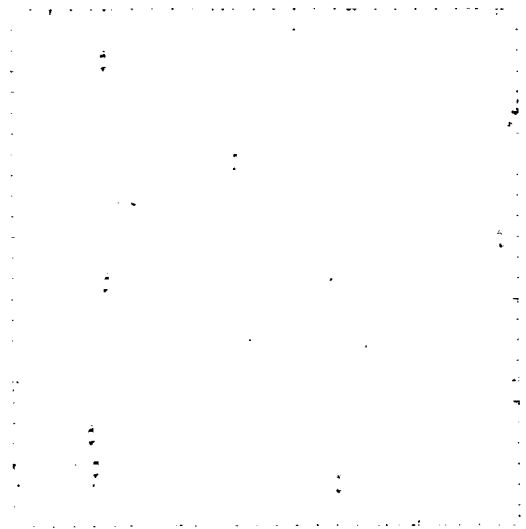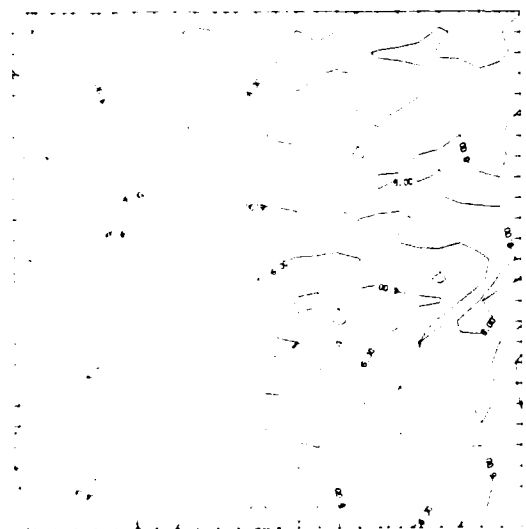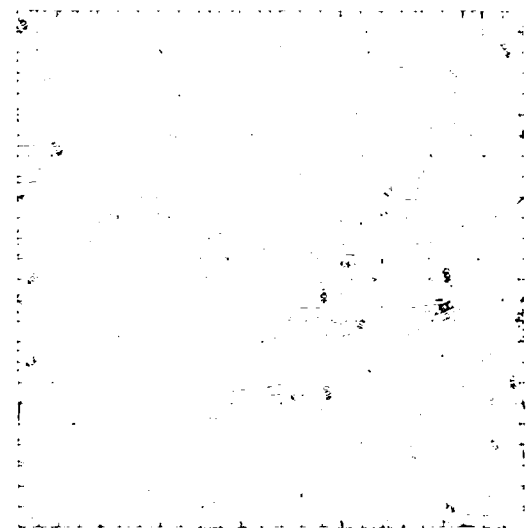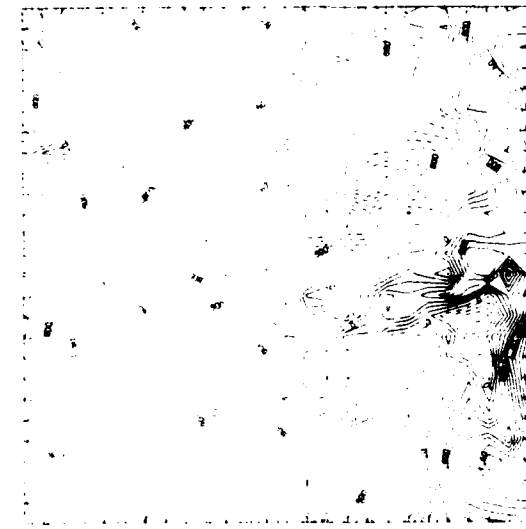
Figure 9. Effect of Blending Surface Data With Rawinsonde Data for Temperature (°C) at About 150 m

18
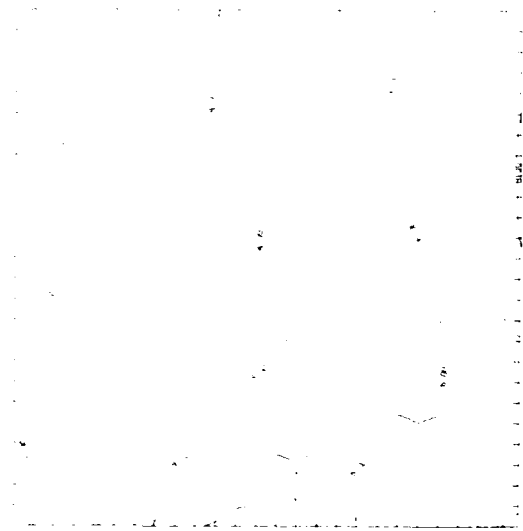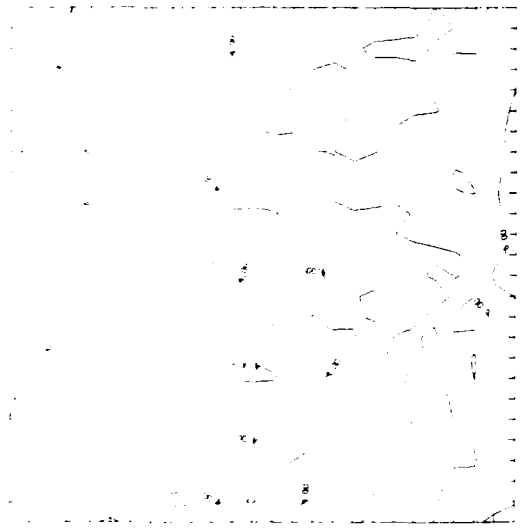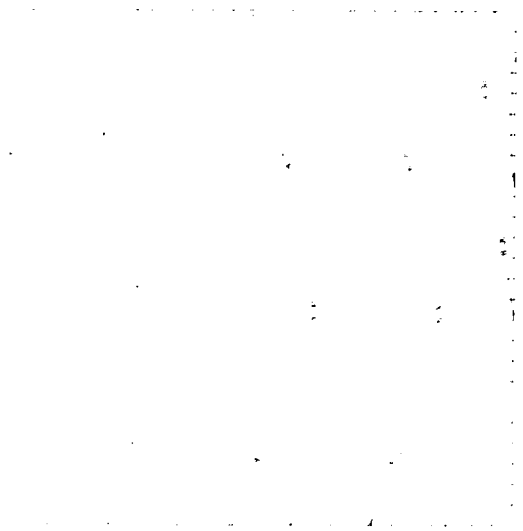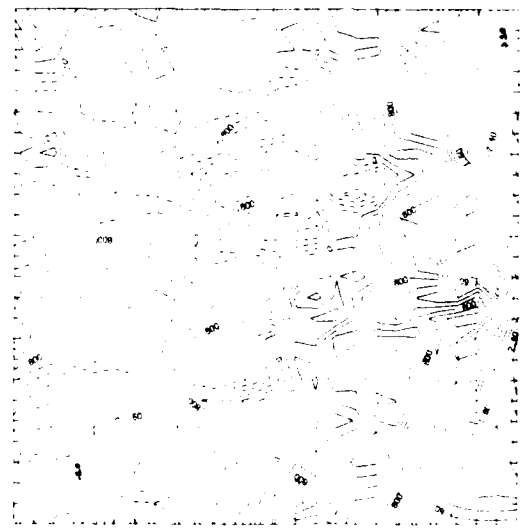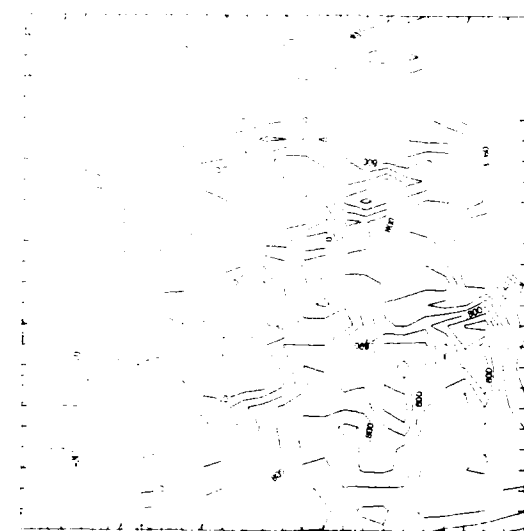
Figure 10. Effect of Blending Surface Data With Rawinsonde Data for Temperature (°C) at About 150 m
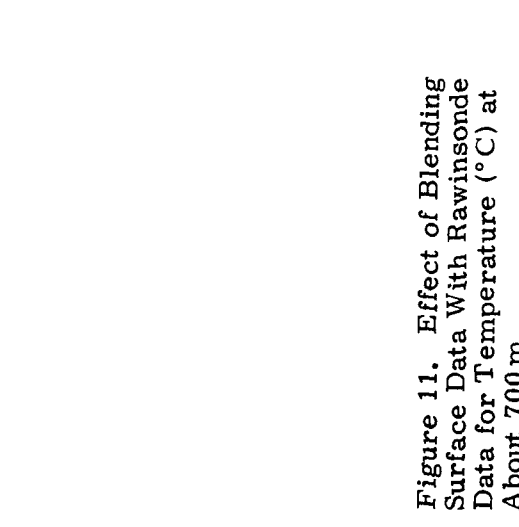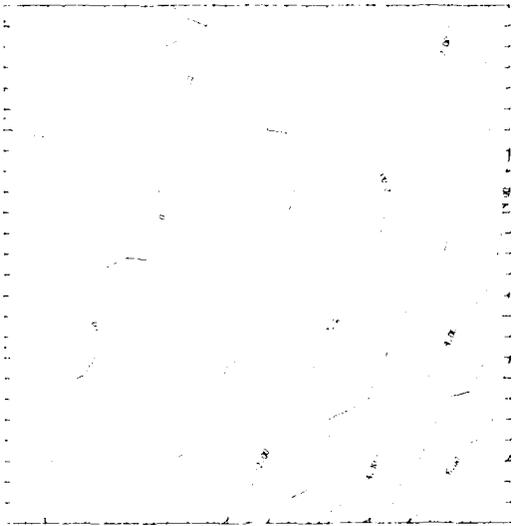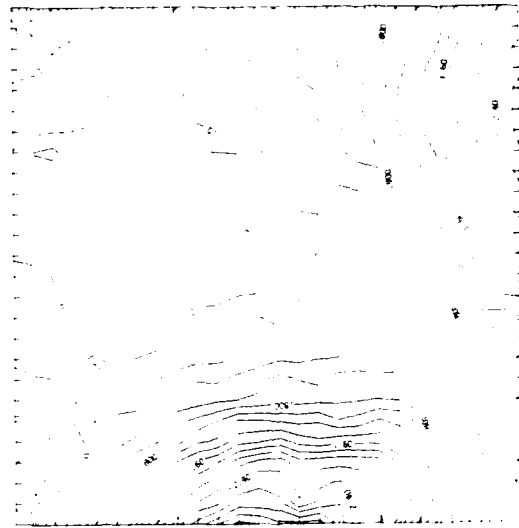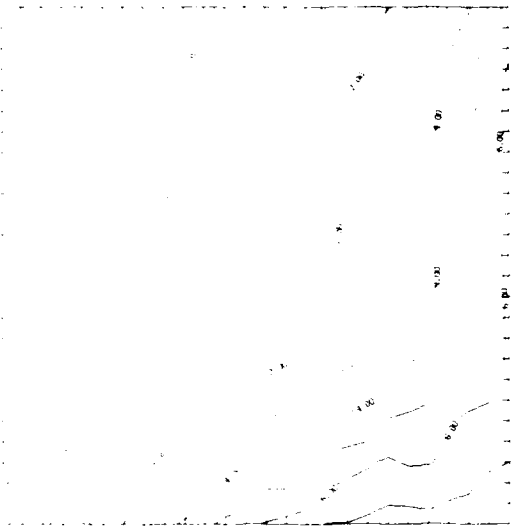
Figure 11. Effect of Blending Surface Data With Rawinsonde Data for Temperature (°C) at About 700 m
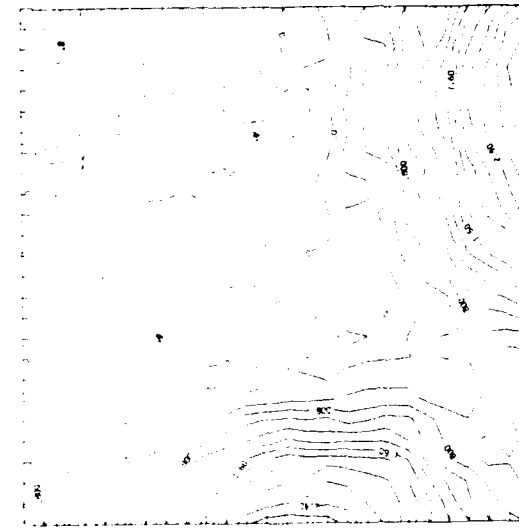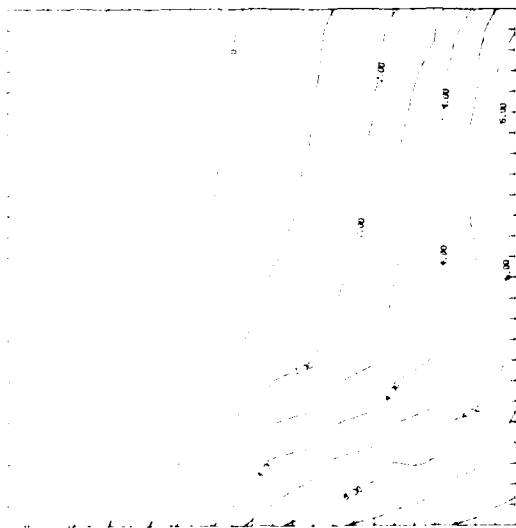
gradient, the blended analysis is more realistic in small-scale features, in amplitudes, and in north-south gradients, as can be seen in the error fields given in panels D and E. From panels D and E, we see also that the blended analysis has a positive bias with a maximum local error on the order of 2° C near the southeastern corner of the domain, whereas the unadjusted analysis has local errors ranging from about -2° C to over 3° C. The blended analyses of q, u, and v show similar trends; thus, only analyses at about 150 m above the ground are shown in Figures 12, 13, and 14, respectively.

For a quantitative comparison of improvements due to the blending technique, we tabulated a set of statistics in Tables 2, 3, 4, and 5 for T, q, u, and v, respectively. Statistics given are the layer-mean-value of the blended analysis, the

Table 2. Comparison Between Blended and Unadjusted
Temperature Analyses

$\bar{p}$ (mb)	$\bar{T}$ (C)	RMSE	MAE	BIAS
850	1.34	0.62 (0.62)	0.40 (0.45)	0.11 (0.03)
897	2.04	1.01 (1.02)	0.68 (0.76)	0.59 (0.38)
935	3.25	1.06 (1.12)	0.81 (0.84)	0.77 (0.44)
963	4.49	0.80 (1.14)	0.63 (0.89)	0.56 (0.08)
977	5.29	0.34 (1.19)	0.25 (1.00)	0.10 (-0.51)
979	5.45	0.28 (1.24)	0.21 (1.05)	0.06 (-0.61)

Table 3. Comparison Between Blended and Unadjusted
Specific Humidity Analyses

$\bar{p}$ (mb)	$\bar{q}$ (g/kg)	RMSE	MAE	BIAS
850	4.64	0.36 (0.41)	0.25 (0.29)	0.07 (0.13)
897	4.54	0.49 (0.52)	0.32 (0.32)	0.12 (0.12)
935	4.71	0.34 (0.41)	0.25 (0.30)	0.13 (0.07)
963	5.02	0.17 (0.36)	0.13 (0.29)	0.09 (-0.03)
977	5.27	0.09 (0.40)	0.07 (0.33)	0.01 (-0.17)
979	5.30	0.07 (0.43)	0.05 (0.35)	0.01 (-0.27)
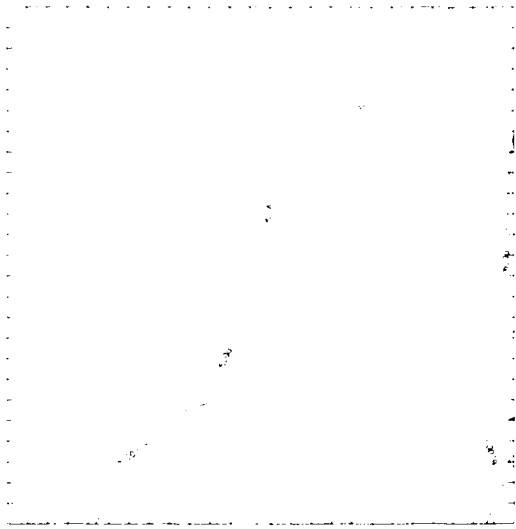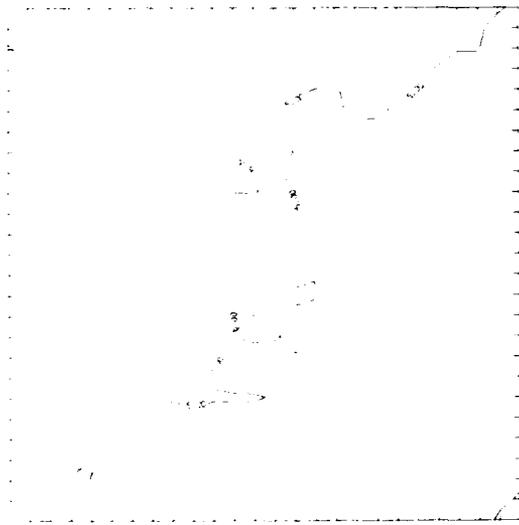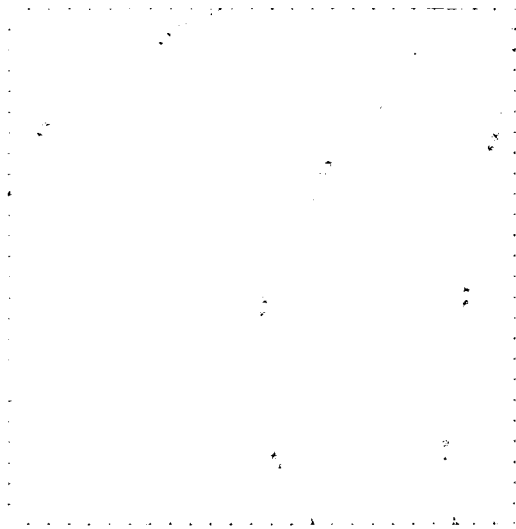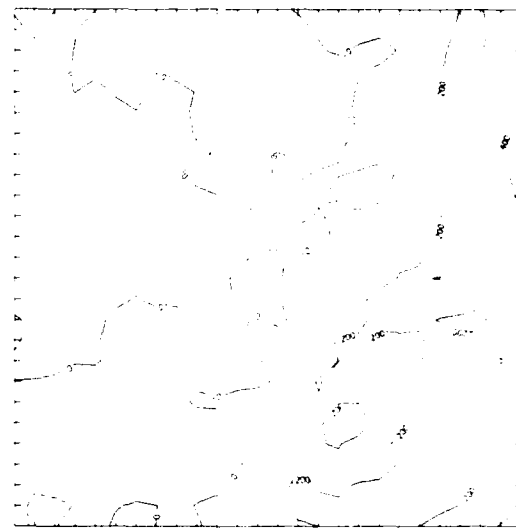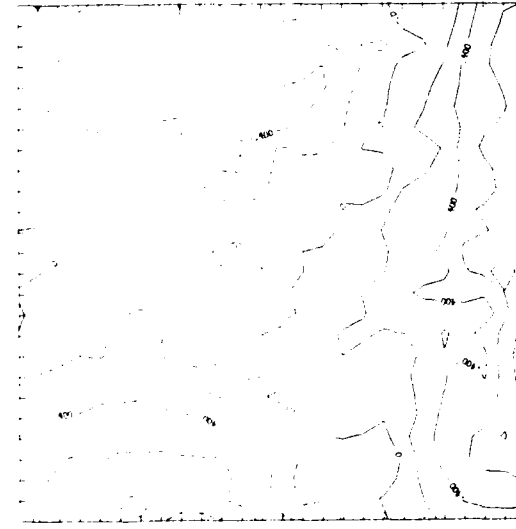
Figure 12. Effect of Blending
Surface Data With Rawinsonde
Data for q (g/kg)

C

E

B

A

D

22
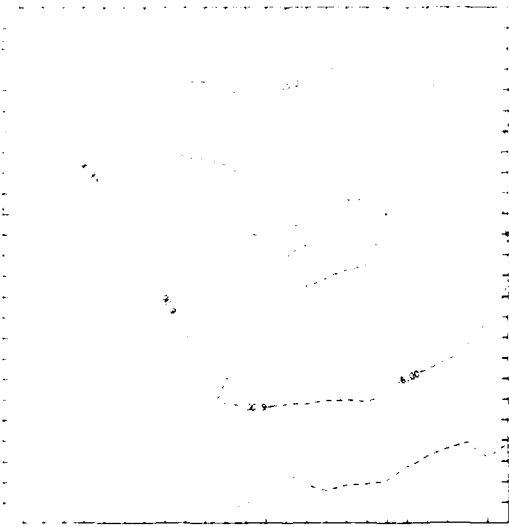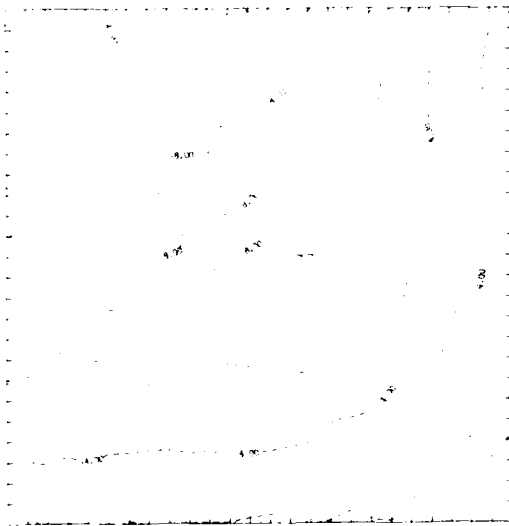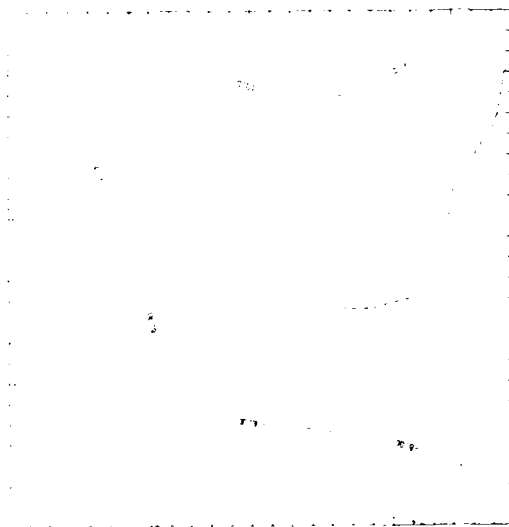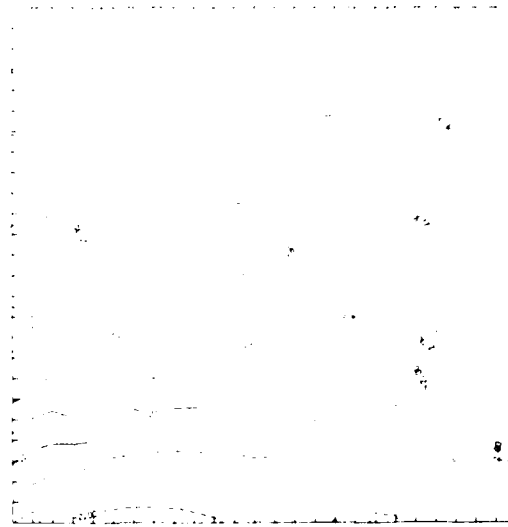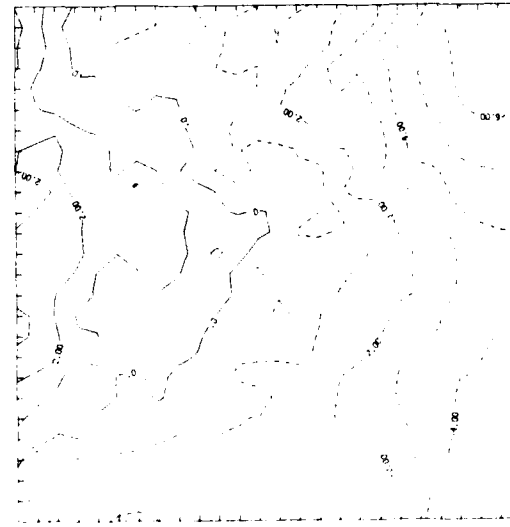
Figure 13. Effect of Blending Surface Data With Rawinsonde Data for u (m/s)
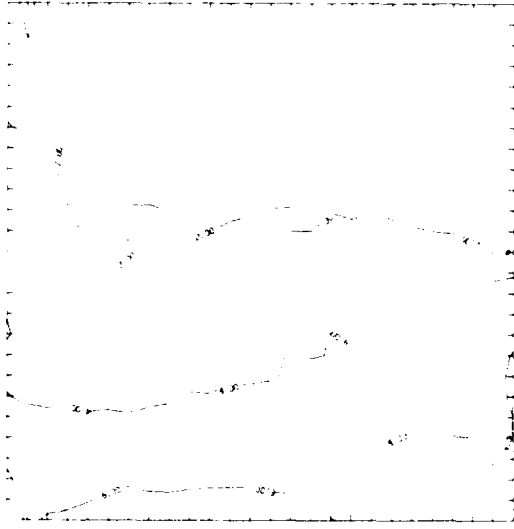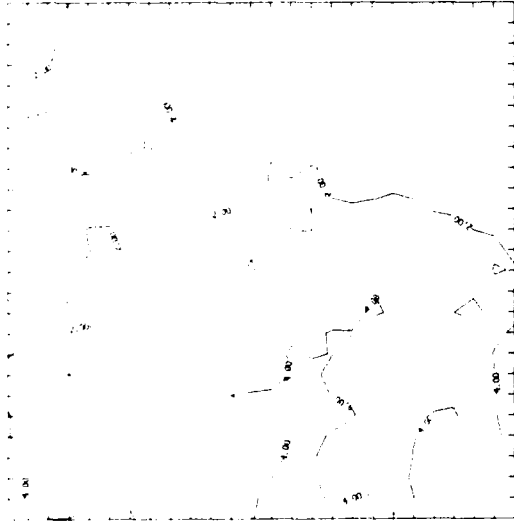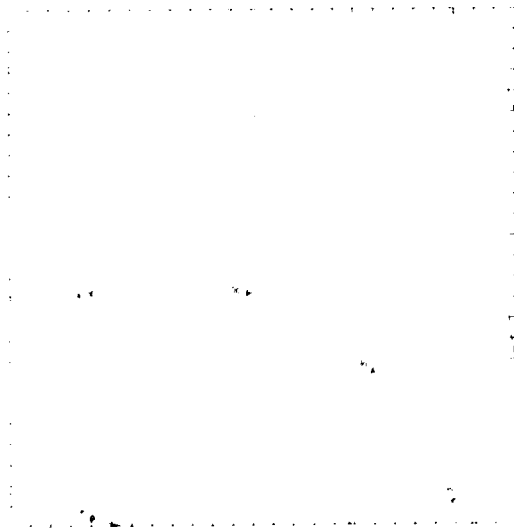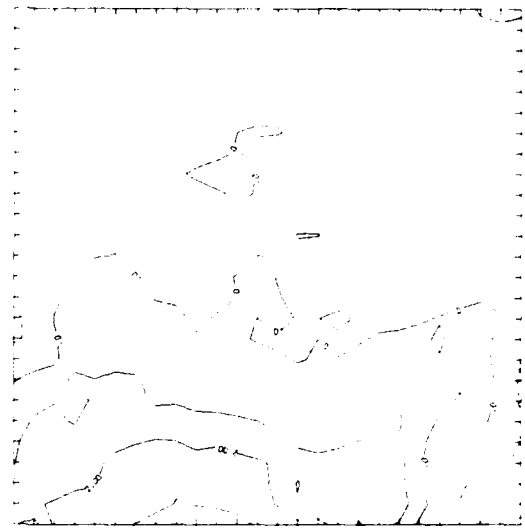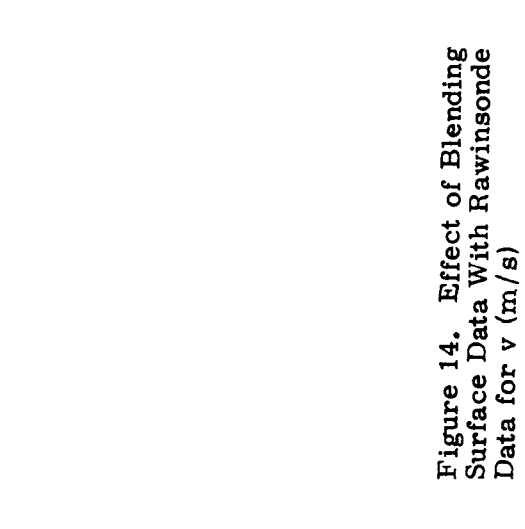
Figure 14. Effect of Blending Surface Data With Rawinsonde Data for v (m/s)

24

Table 4. Comparison Between Blended and Unadjusted u Analyses

$\bar{p}$ (mb)	$\bar{u}$ (m/sec)	RMSE	MAE	BIAS
850	-1.52	2.71 (2.93)	2.24 (2.34)	-2.23 (-1.66)
897	-6.31	2.70 (3.24)	2.06 (2.57)	-1.17 (-0.86)
935	-7.54	2.50 (3.01)	1.95 (2.30)	-1.16 (-1.10)
963	-6.84	2.01 (2.57)	1.68 (2.01)	-1.22 (-1.42)
977	-4.51	0.73·(1.86)	0.57 (1.59)	-0.39 (-0.83)
979	-3.81	0.58 (1.89)	0.40 (1.65)	-0.05 (-0.63)

Table 5. Comparison Between Blended and Unadjusted v Analyses

$\bar{p}$ (mb)	$\bar{v}$ (m/sec)	RMSE	MAE	BIAS
850	8.57	1.96 (2.09)	1.53 (1.66)	-0.45 (-0.19)
897	6.19	2.90 (2.40)	2.29 (1.77)	-1.89 (-1.36)
935	3.66	2.06 (1.46)	1.72 (1.03)	-1.34 (-0.54)
963	2.31	1.20 (1.63)	0.91 (1.17)	-0.22 (+0.84)
977	0.73	0.64 (2.13)	0.44 (1.72)	+0.10 (+1.43)
979	0.33	0.50 (2.12)	0.33 (1.74)	0.06 (+1.41)

root-mean-square error (RMSE), the mean absolute error (MAE), and the bias--
for the lowest layers of the model where we applied the blending. The correspond-
ing statistics for the unadjusted analyses are given in parentheses. We see that,
with the exception of v, all blended analyses show improvements in terms of
RMSE and MAE. As expected, improvements are largest at the ground and de-
crease with increasing distance from the ground, consistent with the specification
of W_k we used in Eq. (4). In terms of the bias, the blending reduces the negative
bias near the ground but increases the positive bias in the upper part of the blend-
ing region, due to a reversal with height of the bias in the 7-station analysis. For
example, the 7-station analysis is too cold and too dry (in terms of q, not relative
humidity) near the ground but too warm and too wet in the upper part of the blend-
ing region. Since one of the constraints in our method dictates that the elevation-

adjusted analysis for the denser network be adopted as the blended analysis at the ground; in this case, our procedure simply raises both the temperature and the moisture content in the entire blending depth, the magnitude of the increase depending on the distance from the ground. As a result, there is an added positive bias in temperature and moisture in the upper layers of the region. This effect can be seen most readily by comparing analyses and their error fields from layer to layer. Such a set of analyses has been given for the temperature in Figures 9, 10, and 11, where one can track the reversal of the bias with height in the unadjusted analysis (panel D) and the increase of the bias with height in the blended analysis (panel E). It should be emphasized that, with the exception of v in the uppermost two blending layers, the MAE and the RMSE are smaller for the blended analysis even in cases where the magnitude of the bias has been increased by the blending. This is an important point because it indicates that horizontal gradients are weaker and horizontal scales are larger in all the error fields of the blended analyses.

Since the blending did not seem to work well for v in the upper layers, we decided to rerun the procedure for the winds, this time assuming that the surface influence stops at layer 4 on the speculation that, for this data set, the topographical effects on horizontal winds are more or less mechanical and fall-off more rapidly with height than do those on temperature and moisture. The statistics for these runs are contrasted in Tables 6 and 7 with the corresponding statistics from the earlier runs (in parenthesis). We see that, at least for this one case, the latter runs seem to yield better analyses than the earlier runs. Such a comparison suggests that we can fine-tune the blending method by distributing along the vertical the bias at the ground in ways different from that of the present approach.

5. SUMMARY AND DISCUSSION

We have brought to focus the concept of gleaning information from different sets of incomplete and complementary data to obtain a more accurate picture of the state of the atmosphere near the Earth's surface. Using the March 1982 AVE/VAS special network data as the basis for evaluation, we have demonstrated the validity of this concept in one specific application: the blending of surface and rawinsonde data to recover, in mesoscale analyses, the often untapped small-scale signals in the surface data. Our results indicate that even a simple way of blending improves analyses in the boundary layer. Although we tested our concept with only a given method for a single case, it is our belief that the concept has general applicability. Based on the results of this study, we are able to offer the following comments.

Table 6. Comparison of Blended u Analyses for Two Sets of W_k

$\bar{p}$ (mb)	$\bar{u}$ (m/sec)	RMSE	MAE	BIAS
935	-7.16	2.74 (2.50)	2.07 (1.95)	-0.78 (-1.16)
963	-6.61	2.00 (2.01)	1.63 (1.68)	-1.00 (-1.22)
977	-4.43	0.70 (0.73)	0.54 (0.57)	-0.31 (-0.39)
979	-3.81	0.58 (0.58)	0.40 (0.40)	-0.05 (-0.05)

Table 7. Comparison of Blended v Analyses for Two Sets of W_k

$\bar{p}$ (mb)	$\bar{v}$ (m/sec)	RMSE	MAE	BIAS
935	4.25	1.21 (2.06)	1.00 (1.72)	-0.74 (-1.34)
963	2.66	0.93 (1.20)	0.65 (0.91)	+0.13 (-0.22)
977	0.85	0.62 (0.64)	0.45 (0.44)	+0.22 (+0.10)
979	0.33	0.50 (0.50)	0.33 (0.33)	-0.06 (-0.06)

There are limitations and drawbacks of the particular method we tested. First of all, we have assumed that the mesoscale structure in the boundary layer is related solely to the mesoscale structure at the ground. Then we have to adopt a vertical weighting function, perhaps through empirical means, in order to blend signals in the denser surface-station network data with analyses in the boundary layer. An example of the empirical nature of this presents itself in Section 4, where we find it desirable to use different vertical weighting for different atmospheric parameters. Furthermore, our merging technique, as presented, introduces a systematic bias in the blending layer. The sign of the bias is the same as the sign of $\bar{D}$, the domain average of $D_{i,j}$ in Eq. (3). Although this is not a serious problem, it may be dealt with only empirically. For example, instead of forcing the 7-station analysis to coincide with the 21-station analysis at the ground and thus changing the layer mean value of the 7-station analysis by $W_k\bar{D}$, we could add a term $-W_k\bar{D}$ to Eq. (3) so that the layer mean $\bar{T}_k$ remains unchanged; or we could add a term $(1 - \sum_k W_k)\bar{D}(\nu_k - \nu_{k+1})/(1 - \nu_{L+1})$ so that the mean value for the entire blending depth changes only by $\bar{D}$. Nevertheless, there is no unique way of blending the two sets of data.

As mentioned earlier, the use of surface data has been avoided until recent years due to the strong topographical effect on atmospheric variables near the ground and the rapid variation of topography in some regions of the globe. However, what is considered to be noise in large-scale modeling may well be the very signals that mesoscale modelers seek. In terms of representativeness of surface data, mesoscale modelers must weigh the error due to omission against the error due to nonrepresentativeness. In terms of the rapid variation of an atmospheric variable with height near the ground, we have demonstrated that, to a large extent, the vertical component of the variation can be reconstructed by extrapolation/interpolation from the analyzed to the archived topography. We wish to emphasize here that a σ-surface analysis for N pieces of input data should be measured against an analysis of the station elevations for the same N reporting stations; and that the analyzed topography, especially when the number of reporting stations is small, may be very different from the archived topography, as was clearly illustrated in Figure 2.

The problem of visual display of surface analyses of atmospheric variables is indeed a problem. However, in addition to sea-level maps, we recommend the display of weather maps in the form of surface tendency analysis. As long as diurnal variations of a parameter can be removed easily, such as in the cases of temperature and pressure, a map of tendencies may indeed provide more insight to the short-term mesoscale weather changes than a map of the parameter itself.

We do not consider this study to be an observing system experiment (OSE) because it has not been our goal to assess whether data from an additional observing system (in this case, the added surface observations) will impact positively on a given analysis algorithm. Rather, we presumed that the additional surface data, when incorporated properly, will have a beneficial impact on the accuracy of the boundary layer analyses. Our goal has been to demonstrate that a simple approach of linearly combining separate analyses of data from different observing systems may well be an efficient way of getting more accurate analyses. A side benefit of our study is that it heightens our awareness of the difficulties in separating the sources of impact in OSE's. Just as in the case of data analysis in which the impact of additional data depends on both the nature of the new data and the way these data are incorporated, the impact of the added data in an OSE also depends on both the characteristics of the added data and those of the assimilation-prediction-verification (A-P-V) system. For example, if the given A-P-V system is insensitive to the resolution of data, it is unlikely that any amount of added high resolution data will have measurable impact on the forecasts. On the other hand, if we redesign the A-P-V system so that it is responsive to the characteristics of the new data set, we undoubtedly will find that the added data have an impact on the forecasts.

Finally, we must reiterate that the blending technique given by Eq. (4) is probably among the simplest. More sophisticated techniques may yield more representative results. In fact, it is a simple matter, for example, if satellite data are available, to add a term in Eq. (4) to incorporate the difference-field between an analysis using only satellite data and that using only rawinsonde data. We recognize that the idea of making use of data from all available sources has been implemented operationally for many years. What we wish to advocate here is the idea of analyzing independent sets of data separately and then merging these analyses in some consistent manner, an idea akin to that of improving forecast accuracy by combining independent forecasts.[9]

---

9. Thompson, P. D. (1977) How to improve accuracy by combining independent forecasts. Mon, Wea, Rev, 105:228-229.

References

1. Nickerson, E. C. (1979) On the numerical simulation of airflow and clouds over mountainous terrain, Beit. zur Physik der Atmos. 52:161-177.

2. Perkey, D. J. (1976) A description of preliminary results from a fine-mesh model for forecasting quantitative precipitation. Mon. Wea. Rev. 104:1513-1526.

3. DiMego, G. J. (1988) The National Meteorological Center regional analysis system, Mon. Wea. Rev. (in press).

4. Golding, B. W. (1987) Strategies for using mesoscale data in an operational mesoscale model, in Mesoscale Analysis and Forecasting. Proc. IAMAP/WMO/ESA, Vancouver, Canada, pp. 569-578.

5. Gustafsson, N. (1987) Opportunities and problems in mesoscale analysis, in Mesoscale Analysis and Forecasting. Proc. IAMAP/WMO/ESA, Vancouver, Canada, pp. 555-560.

6. Kalb, M. W. (1984) Initialization of a mesoscale model for April 10, 1979, using alternative data sources. NASA Contractor Report 3826, NASA, D. C. 20456.

7. Scienkiewicz, M. E. (1982) AVE/VAS III: 25 mb Sounding Data. NASA Contractor Report 170692, NASA, D. C. 20456.

8. Muench, H. S., and Chisholm, D. A. (1985) Aviation Weather Forecast Based on Advection: Experiments Using Modified Initial Conditions and Improved Analyses. AFGL-TR-85-0011, AD A160369.

9. Thompson, P. D. (1977) How to improve accuracy by combining independent forecasts. Mon. Wea. Rev. 105:228-229.